Multiscale and Multiphysics Mechanics, *Vol. 1, No. 1 (2016) 15-33*
DOI: http://dx.doi.org/10.12989/mmm.2016.1.1.015

An asymptotic multi-scale approach for beams via strain gradient elasticity: surface effects

Jun-Sik Kim*

Department of Mechanical System Engineering, Kumoh National Institute of Technology, 61 Daehak-ro, Gumi, Gyeongbuk 730-701, Republic of Korea

(Received May 1, 2015, Revised October 5, 2015, Accepted October 6, 2015)

Abstract. In this paper, an asymptotic method is employed to formulate nano- or micro-beams based on strain gradient elasticity. Although a basic theory for the strain gradient elasticity has been well established in literature, a systematic approach is relatively rare because of its complexity and ambiguity of higher-order elasticity coefficients. In order to systematically identify the strain gradient effect, an asymptotic approach is adopted by introducing the small parameter which represents the beam geometric slenderness and/or the internal atomistic characteristic. The approach allows us to systematically split the two-dimensional strain gradient elasticity into the microscopic one-dimensional through-the-thickness analysis and the macroscopic one-dimensional beam analysis. The first-order beam problem turns out to be different from the classical elasticity in terms of the bending stiffness, which comes from the through-the-thickness strain gradient effect. This subsequently affects the second-order transverse shear stress in which the surface shear stress exists. It is demonstrated that a careful derivation of a first strain gradient elasticity embraces "Gurtin-Murdoch traction" as the surface effect of a one-dimensional Euler-Bernoulli-like beam model.

Keywords: strain gradient elasticity; size effect; surface tension; asymptotic method

1. Introduction

A strain gradient elasticity theory has a long history, and there have been many research works up to days. It has been known that the theory is able to handle various size-effects in different applications such as crack tip stress singularity, dislocations, porous materials, and surface tension, etc. For the purpose of a systematic asymptotic formulation, a first strain gradient elasticity addressed by Mindlin (1964) is treated in this paper.

A strain gradient elasticity (Mindlin 1964, 1965) belongs to the wide definition of nonlocal elasticity that is named in contrast to the local elasticity (or classical elasticity). The generalized Hooke's law is obeyed at a material point in the local elasticity, whereas it may not be applied to the nonlocal elasticity. The stress at a material point is affected by a stress state near the point in the nonlocal elasticity (Eringen 1983, 2002). As a nanotechnology is evolved, a nonlocal elasticity is paid attention to relevant society. A major reason of this is that molecular dynamics and/ or quantum mechanics based simulations require tremendous computation resources (Kim and Cho

*Corresponding author, Professor, E-mail: junsik.kim@kumoh.ac.kr

 ISSN: 2383-7306 (Print), 2465-9711 (Online)

2010). A three-dimensional approach for such a nonlocal elasticity is not a viable option, because it also takes a lot of computational efforts. Therefore there have been many research works for developing beam/plate models based on various nonlocal elasticity theories, which may be categorized into three groups: Eringen's (1983, 2002) simplified nonlocal elasticity, a strain gradient elasticity (Mindlin 1964, 1965), and Gurtin and Murdoch's (1975, 1978) surface elasticity.

1.1 Eringen's simplified nonlocal elasticity based models

A first application of Eringen's nonlocal elasticity to beam models is possibly the work of Peddieson *et al.* (2003), where they included the axial stress gradient effect only to derive an Euler-Bernoulli-like beam model. There have also been Timoshenko-like beam models in order to solve many problems, such as dynamic dispersion, vibration, and buckling (Wang *et al.* 2006, Reddy 2007). The recent work of Kim (2014a) revealed that a nonlocal Euler-Bernoulli-like beam model is equivalent to a local Rankine-Timoshenko beam model. The nonlocal effect makes the beam softer, since it is analogous to the shear deformation in a local Rankine-Timoshenko beam model. Nonlocal higher-order bam theories have been studied by Reddy (2007), the results obtained therein indicated that all the higher-order theories show a softening behavior.

1.2 Strain gradient elasticity based models

In this category, most popular form is a couple stress theory that stems from a strain gradient elasticity. Yang *et al.* (2002) employed and modified a first strain gradient elasticity in order to have one material length parameter for a linear isotropic elasticity. For a flat plate of infinite width, the strain gradient effect shows that a bending rigidity increases as the thickness of the plate decreases (stiffening behavior). This work is extended to a higher-order displacement-based model for a plane strain cantilever (Lam *et al.* 2003). The result obtained therein is compared to the experiment, which shows a stiffening behavior. Ma *et al.* (2008) developed a Timoshenko beam model based on the modified couple stress theory proposed by Yang *et al.* (2002). They solved the static and dynamic problems of a simply-supported beam. The result obtained indicates a stiffening behavior. For all the works mentioned in above, they used a three-dimensional relationship directly without applying any proper conditions, and their solutions rely upon the assumed displacement fields. This may lead to an inconsistent beam model with a classical beam model. For instance, in the work of Ma *et al.* (2008), they have to set the Poisson's ratio to be zero in order to recover a classical beam model. In a classical elasticity, an Euler-Bernoulli beam model has a simple constitutive relation $\sigma=E\varepsilon$ that can be systematically derived from a classical three-dimensional elasticity by applying plane stress conditions to the cross-sectional coordinates of the beam. It is not necessary to have a special condition like the zero Poisson's ratio.

1.3 Gurtin and Murdoch's surface elasticity based models

It has been well known that the surface effect plays a crucial role in nano-sized elastic bodies. Many researches have been carried out by using molecular dynamics-based simulations. There has also been an effort to explain the effect based on a continuum mechanics approach. Gurtin and Murdoch (1975, 1978) proposed the surface model by introducing the initial surface stress and surface Lame constants. Lim and He (2004) employed the Gurtin and Murdoch's surface model to

formulate the beam/plate models in order to consider a size-effect. Lu *et al.* (2006) modified Lim and He's approach by including the transverse normal stress contribution, and they arrived at the different bending stiffness. Kim (2014b) derived a nonlocal Euler-Bernoulli beam model from the Eringen's simplified model by considering the thickness stress gradient effect. The nonlocal transverse shear stress is derived from a nonlocal stress equilibrium equation, and the unknowns therein are found by applying the top and bottom surface conditions. He arrived at a similar bending stiffness model to Lu *et al*. (2006) except for the nonlocal parameter.

On the other hand, there have been continuum-based bridging models, where the surface parameters are found by a molecular dynamics (MD) simulation. Cho *et al.* (2009) proposed a sequential multi-scale method to determine the surface constants using a matching method based on a MD simulation. The method is extended to nano-film and nano-wire with the consideration of anisotropic surfaces (Kim *et al.* 2012). They pointed out that the surface constitutive equation based approach could be problematic as applied to non-rectangular cross-sectional shapes.

A brief review of literature is made in the above, although it does not cover the entire body of research works. In literature, one can find some interesting works, such as second strain gradient elasticity (Lazar *et al.* 2006, Polizzotto 2012), variational frame work for gradient elasticity theories (Polizzotto 2003, 2015, Paola *et al.* 2010), and gradient elasticity reviews (Askes and Aifantis 2011).

The objective of this paper is to systematically develop a nano-beam model by applying a formal asymptotic method (Kim *et al.* 2008, Kim 2009, Kim and Wang 2011) to a first strain gradient elasticity. In this way, one can asymptotically incorporate the thickness length scale effect into a macroscopic beam model and predict the through-the-thickness stress distributions with the residual surface tension. To this end, we scale the free energy by introducing the small parameters associated with geometric slenderness and internal characteristic length. This allows one to split a three-dimensional problem into two dimensionally reduced problems, such as microscopic sectional and macroscopic beam problems. The warping displacements are obtained by solving the microscopic sectional problem, which are substituted back into the macroscopic beam problem. The resulting beam model is equipped with an asymptotically correct beam stiffness. Once we solved the macroscopic beam problem, its solution can be used to calculate the stress distributions through the thickness of the beam. As numerical examples, a cantilever beam configuration is selected as a test-bed, it is shown that the surface effect has an impact on local stress distributions as well as global responses.

2. A first strain graient elasticity

A two-dimensional beam-like isotropic elastic body is considered by employing the plane stress condition. The beam length is denoted by x_1, the thickness by x_3, and the beam width (b) is constant. A free energy for a first strain gradient elasticity is adopted, which is suitable for practical engineering applications, to derive nano- and/or micro-beam models. That is

$$U = \frac{1}{2}\left(\boldsymbol{\gamma}^T \mathbf{C}\boldsymbol{\gamma} + a_0 \boldsymbol{\gamma}_{,k}^T \mathbf{C}\boldsymbol{\gamma}_{,k}\right) \tag{1}$$

where a_0 is an internal characteristic scale parameter, which can be approximately obtained by using the kernel function, the dispersion curve of the Born-Karman model (Eringen 2002), and the

molecular dynamic simulation (Cho *et al*. 2009). The linear elasticity matrix is denoted by $\mathbf{C}$, and the linear strain vector $\boldsymbol{\gamma}$ is given by

$$\boldsymbol{\gamma} = \lfloor \gamma_{11} \quad \gamma_{33} \quad 2\gamma_{13} \rfloor^T, \ \gamma_{11} = u_{1,1}, \ \gamma_{33} = u_{3,3}, \ 2\gamma_{13} = u_{1,3} + u_{3,1} \tag{2}$$

2.1 Asymptotic formulation

In order to apply the asymptotic expansion method by taking the advantage of the beam geometric slenderness, one needs to define the small parameter (ε) which is defined by the ratio of the beam thickness (h) to the beam characteristic length (l_c). The beam coordinates are then scaled as

$$y_1 = x_1, \ y_3 = x_3/\varepsilon, \ \varepsilon \equiv h/l_c \tag{3}$$

and the internal characteristic scale parameter a_0 is very small, thus it is reasonable to scale it in the following manner

$$a_0 = a_0 \left(h/l_a\right)^2 \left(l_a/h\right)^2 = \bar{a}_0 \varepsilon^2, \ \varepsilon \sim la/h \tag{4}$$

where l_a is the internal characteristic length, which is the order of the Fermi wave length or a lattice constant and less than 1nm, in general.

Substituting Eqs. (3)-(4) into Eq. (1) yields the scaled free energy as follows

$$U = \frac{1}{2}\varepsilon \int_{y_3^-}^{y_3^+} \left(\boldsymbol{\gamma}^T \mathbf{C} \boldsymbol{\gamma} + \bar{a}_0 \boldsymbol{\gamma}_{,3}^T \mathbf{C} \boldsymbol{\gamma}_{,3} + \varepsilon^2 \bar{a}_0 \boldsymbol{\gamma}_{,1}^T \mathbf{C} \boldsymbol{\gamma}_{,1} \right) dy_3 \tag{5}$$

Taking the first variation of Eq. (5) gives

$$\delta U = \varepsilon \int_{y_3^-}^{y_3^+} \left(\left(\delta \boldsymbol{\gamma}\right)^T \mathbf{C} \boldsymbol{\gamma} + \bar{a}_0 \left(\delta \boldsymbol{\gamma}_{,3}\right)^T \mathbf{C} \boldsymbol{\gamma}_{,3} + \varepsilon^2 \bar{a}_0 \left(\delta \boldsymbol{\gamma}_{,1}\right)^T \mathbf{C} \boldsymbol{\gamma}_{,1} \right) dy_3 \tag{6}$$

The linear strain vector can be scaled by using Eq. (3). That is

$$\boldsymbol{\gamma} = \lfloor u_{1,1} \quad 0 \quad u_{3,1} \rfloor^T + \left(1/\varepsilon\right) \lfloor 0 \quad u_{3,3} \quad u_{1,3} \rfloor^T \tag{7}$$

To complete the formulation, the displacement is now expanded by the small parameter. Then the asymptotic expansion of the displacement vector is given by

$$\mathbf{u} = \lfloor u_1 \quad u_3 \rfloor^T = \mathbf{u}^{(0)} + \varepsilon \mathbf{u}^{(1)} + \varepsilon^2 \mathbf{u}^{(2)} + \varepsilon^3 \mathbf{u}^{(3)} + \cdots \tag{8}$$

where the right hand side terms in Eq. (8) are unknowns but the zeroth-order displacement vector that has the form of

$$\mathbf{u}^{(0)} = \lfloor 0 \quad v_3^{(0)} \rfloor^T \tag{9}$$

in which the displacement component $v_i^{(n)}$ is a function of the axial coordinate y_1 only.

The strain vector, by substituting Eq. (8) into Eq. (7), is then expanded as follows

$$\boldsymbol{\gamma} = \boldsymbol{\gamma}^{(0)} + \varepsilon\boldsymbol{\gamma}^{(1)} + \varepsilon^2\boldsymbol{\gamma}^{(2)} + \varepsilon^3\boldsymbol{\gamma}^{(3)} + \cdots \tag{10}$$

where the zeroth-order strain vector is given by

$$\boldsymbol{\gamma}^{(0)} = \begin{bmatrix} 0 & 0 & v_{3,1}^{(0)} \end{bmatrix}^T + \begin{bmatrix} 0 & u_{3,3}^{(1)} & u_{1,3}^{(1)} \end{bmatrix}^T \tag{11}$$

Once the strain vector is asymptotically expanded, the local stress vector $\boldsymbol{\sigma}$ can be also expanded by the Hooke's law.

The free energy can be asymptotically expanded, when the strain vector is expanded. Substituting Eq. (10) into Eq. (6). The first variation of the free energy is expanded as follows

$$\delta U = \varepsilon\delta U^{(0)} + \varepsilon^2\delta U^{(1)} + \varepsilon^3\delta U^{(2)} + \varepsilon^4\delta U^{(3)} + \cdots \tag{12}$$

The zeroth-order energy variation can be summarized by

$$\delta U^{(0)} = \int_{y_3^-}^{y_3^+} \left(\left(\delta\boldsymbol{\gamma}^{(0)}\right)^T \mathbf{C}\boldsymbol{\gamma}^{(0)} + \bar{a}_0 \left(\delta\boldsymbol{\gamma}_{,3}^{(0)}\right)^T \mathbf{C}\boldsymbol{\gamma}_{,3}^{(0)} \right) dy_3 \tag{13}$$

The problem is well-posed, thus one can set the energy to be zero (Kim *et al.* 2008), i.e., $\boldsymbol{\gamma}^{(0)} = 0$. Form this, we obtain the particular displacement component. Finally adding the rigid-body displacement completes the fundamental displacement vector such that

$$\mathbf{u}^{(1)} = \begin{bmatrix} v_1^{(1)} - y_3 v_{3,1}^{(0)} & v_3^{(1)} \end{bmatrix}^T \equiv \tilde{\mathbf{u}}^{(1)} \tag{14}$$

which makes the first-order strain vector zero.

2.2 First nontrivial warping solutions

The first-order energy variation is automatically satisfied due to the zero first-order strain vector. The first nontrivial displacement vector can be found in the second-order energy which is expressed as

$$\delta U^{(2)} = \int_{y_3^-}^{y_3^+} \left(\left(\delta\boldsymbol{\gamma}^{(1)}\right)^T \mathbf{C}\boldsymbol{\gamma}^{(1)} + \bar{a}_0 \left(\delta\boldsymbol{\gamma}_{,3}^{(1)}\right)^T \mathbf{C}\boldsymbol{\gamma}_{,3}^{(1)} \right) dy_3 \tag{15}$$

Applying the integration by parts through the thickness of the beam yields

$$\delta U^{(2)} = \int_{y_3^-}^{y_3^+} \left(\left(\delta\boldsymbol{\gamma}^{(1)}\right)^T \mathbf{t}^{(1)} \right) dy_3 + \left[\bar{a}_0 \left(\delta\boldsymbol{\gamma}^{(1)}\right)^T \boldsymbol{\sigma}_{,3}^{(1)} \right]_{y_3^-}^{y_3^+} \tag{16}$$

where

$$\boldsymbol{\sigma}^{(1)} = \mathbf{C}\boldsymbol{\gamma}^{(1)}, \quad \mathbf{t}^{(1)} \equiv \boldsymbol{\sigma}^{(1)} - \bar{a}_0\boldsymbol{\sigma}_{,33}^{(1)} \tag{17}$$

in which $\boldsymbol{\sigma}$ obeys the Hooke's law and is referred to as a Cauchy-like stress, while the total stress $\mathbf{t}$ includes the strain gradient (Lazar *et al.* 2006, Polizzotto 2012). Notice here that the nonlocal stress originally contains axial derivative term as well as thickness derivative one, however, due to

the scaling, the thickness derivative term appears only at the first-order nonlocal stress. This implies that the axial derivative term is a higher-order one, indeed, it will be shown later that a surface effect can be captured by the through-the-thickness gradient of the Cauchy-like stress.

To find the second-order displacement vector, we introduce a warping displacement vector (**w**) which can be regarded as a perturbation with respect to the second-order fundamental displacement in such a way that

$$\mathbf{u}^{(2)} = \tilde{\mathbf{u}}^{(2)} + \mathbf{w}^{(2)} \tag{18}$$

which renders the first-order strain vector as

$$\boldsymbol{\gamma}^{(1)} = \begin{bmatrix} v_{1,1}^{(1)} - y_3 v_{3,11}^{(0)} & 0 & 0 \end{bmatrix}^T + \begin{bmatrix} 0 & w_{3,3}^{(2)} & w_{1,3}^{(2)} \end{bmatrix}^T \tag{19}$$

Substituting Eq. (19) into Eq. (16) yields the microscopic equation associated with the variation of warping displacements

$$\begin{aligned} -\int_{y_3^-}^{y_3^+} \left(t_{13,3}^{(1)} \delta w_1^{(2)} + t_{33,3}^{(1)} \delta w_3^{(2)} \right) dy_3 + \left[t_{13}^{(1)} \delta w_1^{(2)} + t_{33}^{(1)} \delta w_3^{(2)} \right]_{y_3^-}^{y_3^+} \\ + \bar{a}_0 \left[\sigma_{13,3}^{(1)} \delta w_{1,3}^{(2)} + \sigma_{33,3}^{(1)} \delta w_{3,3}^{(2)} \right]_{y_3^-}^{y_3^+} = 0 \end{aligned} \tag{20}$$

and the macroscopic equation associated with the variation of the fundamental displacements as

$$\int_{y_3^-}^{y_3^+} \left(t_{11}^{(1)} \delta v_{1,1}^{(1)} - y_3 t_{11}^{(1)} \delta v_{3,11}^{(0)} \right) dy_3 + \bar{a}_0 \left[\sigma_{11,3}^{(1)} \delta v_{1,1}^{(1)} - y_3 \sigma_{11,3}^{(1)} \delta v_{3,11}^{(0)} \right]_{y_3^-}^{y_3^+} = 0 \tag{21}$$

This microscopic equation will be treated in later section.

The first term in Eq. (20) yields general solutions for warping displacements as

$$\begin{aligned} w_1^{(2)} &= c_{11} \cosh\left(\tfrac{y_3}{\sqrt{\bar{a}_0}}\right) + c_{12} \sinh\left(\tfrac{y_3}{\sqrt{\bar{a}_0}}\right) + c_{13} y_3 + c_{14} \\ w_3^{(2)} &= c_{31} \cosh\left(\tfrac{y_3}{\sqrt{\bar{a}_0}}\right) + c_{32} \sinh\left(\tfrac{y_3}{\sqrt{\bar{a}_0}}\right) + c_{33} y_3 + c_{34} + \tfrac{1}{2} \nu y_3^2 v_{3,11}^{(0)} \end{aligned} \tag{22}$$

where ν is the Poisson's ratio. Applying the boundary conditions given in Eq. (20) to Eq. (22) with warping displacements constraints such that

$$\left\langle w_1^{(2)} \right\rangle = \left\langle w_3^{(2)} \right\rangle = 0, \quad \langle \bullet \rangle \equiv \int_{y_3^-}^{y_3^+} \bullet \, dy_3 \tag{23}$$

gives the unknowns in Eq. (22). The explicit forms of the second-order warping displacements are written as follows

$$w_1^{(2)} = 0, \quad w_3^{(2)} = \tfrac{1}{2} \nu \left(y_3^2 - \tfrac{h^2}{12} \right) v_{3,11}^{(0)} - \nu y_3 v_{1,1}^{(1)} \tag{24}$$

The second-order warping displacements make it possible to express the first-order Cauchy-like and total stresses. Then the Cauchy-like stress tensor is obtained as

$$\sigma_{11}^{(1)} = E \left(v_{1,1}^{(1)} - y_3 v_{3,11}^{(0)} \right), \ \sigma_{13}^{(1)} = 0, \ \sigma_{33}^{(1)} = 0, \tag{25}$$

in which E is the Young's modulus, and the total stress tensor is found to be the same as the

Cauchy-like stress tensor in this case. It will however be shown later that they are different in higher-order levels.

2.3 Surface tension as a pre-stress

A nano-beam structure under the surface tension can be regarded as a pre-stressed beam. The presence of the surface tension may be drawn in the zeroth-order free energy. As mentioned in section 2.2, the problem is well posed, thus the zeroth-order strain vector is assumed to be zero. This naturally leads to that the zeroth-order Cauchy-like stress tensor is zero. However one should notice here that there is a Cauchy-like stress tensor while satisfying the zero total stress. Thus the pre-stress state with scaling of ε, which is a function of y_3 only, can be formulated as

$$t_{11}^s = \sigma_{11}^s - \bar{a}_0 \sigma_{11,33}^s = 0 \quad \text{s.t.} \quad \left[\bar{a}_0 \sigma_{11,3}^s \delta v_{1,1} \right]_{y_3^-}^{y_3^+} \tag{26}$$

where the coefficients are subject to the surface stress conditions τ_0^ε which should be scaled. The order of magnitude of the surface tension is presupposed as $\tau_0^\varepsilon = \varepsilon \tau_0$. Then the surface tension is added to the first-order Cauchy-like stress tensor in such a way that

$$\sigma_{11}^{(1)} = E\left(v_{1,1}^{(1)} - y_3 v_{3,11}^{(0)} \right) + \frac{\tau_0}{\sqrt{\bar{a}_0}} \operatorname{csch}\left(\tfrac{h}{2\sqrt{\bar{a}_0}}\right) \cosh\left(\tfrac{y_3}{\sqrt{\bar{a}_0}}\right) \tag{27}$$

which does not alter the total stress due to Eq. (26). It is worthwhile to mention that the total stress tensor is comparable to the local stress tensor in a classical elasticity, whereas the Cauchy-like stress tensor is to the nonlocal stress tensor in a nonlocal elasticity (Lazar *et al.* 2006, Polizzotto 2012).

2.4 First nontrivial macroscopic beam equations

The first nontrivial beam equation can be derived by the macroscopic equation given in Eq. (21). Substituting Eq. (27) into Eq. (21) yields

$$\left[N^{(1)} + 2\tau_0 \right] \delta v_{1,1}^{(1)} + \left[M^{(1)} + \bar{a}_0 E h v_{3,11}^{(0)} \right] \delta v_{3,11}^{(0)} = 0 \tag{28}$$

where

$$N^{(1)} \equiv \left\langle t_{11}^{(1)} \right\rangle, \; M^{(1)} \equiv \left\langle -y_3 t_{11}^{(1)} \right\rangle \tag{29}$$

The definitions of stress resultants are the same as those of local stress resultants, however, Eq. (28) implies that the governing equations are different.

For the axial force equation, the surface tension does not affect the axial stiffness but the applied force. This causes the different behaviour which depends on the direction of an applied force p1 at the free end of the beam (i.e., tension or compression). The equilibrium equation and boundary conditions are summarized as follows

$$N_{,1}^{(1)} = 0, \;\; N^{(1)} + 2\tau_0 = p_1 \;\; \text{or} \;\; \delta v_1^{(1)} = 0 \;\; \text{at} \;\; y_1^{\pm} \tag{30}$$

This yields the axial displacement as

$$v_1^{(1)} = \frac{y_1}{EA}\left[p_1 - 2\tau_0 \right],\ v_{1,11}^{(1)} = 0, \tag{31}$$

which tells us that the magnitude of the displacement depends on the direction of an applied force due to the pre-stress (surface tension). This results in the different magnitude of stress if the beam is subjected to tension or compression.

On the other hand, the bending moment equation is given by

$$M^{*(1)}\delta v_{3,11}^{(0)} = 0,\ \ M^{*(1)} \equiv EI\left[1 + \bar{a}_0 \tfrac{12}{h^2}\right] v_{3,11}^{(0)} \tag{32}$$

in which one can see that the bending stiffness of a first strain gradient elasticity differs from that of a classical elasticity according to the normalized material characteristic parameter. One should note that the bending stiffness is affected by the thickness gradient not the axial gradient. Many researchers have considered the axial gradient only in order to explain and/or derive nano- and/or micro-beam models (Reddy 2007, Askes and Aifantis 2011). The present systematic asymptotic approach reveals that a fundamental size-effect comes from the thickness gradient, which makes the beam stiffer. This is one of the key contributions made in this paper.

3. Higher-order free energy

In the previous section, the first nontrivial warping displacements are derived. Substituting these into the macroscopic equation produces an Euler-Bernoulli-like nonlocal beam model. However the transverse stresses are found to be zeros, and therefore, we are not able to see the size-effect in the stresses. To this end, the higher-order terms in the asymptotically expanded free energy are investigated to explicitly derive the transverse stresses.

3.1 The third-order free energy

The third-order energy variation can be summarized as follows

$$\begin{aligned} \delta U^{(3)} = & \int_{y_3^-}^{y_3^+} \left(\left(\delta \boldsymbol{\gamma}^{(1)}\right)^T \mathbf{t}^{(2)} + \left(\delta \boldsymbol{\gamma}^{(2)}\right)^T \mathbf{t}^{(1)} \right) dy_3 \\ & + \left[\bar{a}_0 \left(\delta \boldsymbol{\gamma}^{(1)}\right)^T \boldsymbol{\sigma}_{,3}^{(2)} + \bar{a}_0 \left(\delta \boldsymbol{\gamma}^{(2)}\right)^T \boldsymbol{\sigma}_{,3}^{(1)} \right]_{y_3^-}^{y_3^+} \end{aligned} \tag{33}$$

Following the same way described in section 2.2, the third-order displacement vector and the second-order strain vector are given as follows

$$\mathbf{u}^{(3)} = \tilde{\mathbf{u}}^{(3)} + \mathbf{w}^{(3)} \tag{34}$$

which renders the first-order strain vector as

$$\begin{aligned} \boldsymbol{\gamma}^{(2)} = & \left\lfloor v_{1,1}^{(2)} - y_3 v_{3,11}^{(1)} \quad 0 \quad 0 \right\rfloor^T \\ & + \left\lfloor 0 \quad w_{3,3}^{(3)} \quad w_{1,3}^{(3)} \right\rfloor^T + \left\lfloor w_{1,1}^{(2)} \quad 0 \quad w_{3,1}^{(2)} \right\rfloor^T \end{aligned} \tag{35}$$

Substituting Eq. (35) into Eq. (33) yields the microscopic and macroscopic equations.

The second nontrivial warping solutions can be found in the microscopic equation that is summarized as follows: the governing equation

$$\left(t_{13,3}^{(2)}+t_{11,1}^{(1)}\right)\delta w_1^{(2)}=0,\ \left(t_{33,3}^{(2)}+t_{13,1}^{(1)}\right)\delta w_3^{(2)}=0, \tag{36}$$

which are subjected to the boundary conditions at top and bottom surfaces such that

$$\begin{aligned}&\left(t_{13}^{(2)}-\bar{a}_0\sigma_{11,13}^{(1)}\right)\delta w_1^{(2)}\Big|_{y_3^-}^{y_3^+}=0,\ \left(t_{33}^{(2)}-\bar{a}_0\sigma_{13,13}^{(1)}\right)\delta w_3^{(2)}\Big|_{y_3^-}^{y_3^+}=0,\\&\left(\bar{a}_0\sigma_{13,3}^{(2)}\right)\delta w_{1,3}^{(2)}\Big|_{y_3^-}^{y_3^+}=0,\ \left(\bar{a}_0\sigma_{33,3}^{(2)}\right)\delta w_{3,3}^{(2)}\Big|_{y_3^-}^{y_3^+}=0,\end{aligned} \tag{37}$$

and the third-order warping displacements are also subjected to the constraints given in Eq. (23). Considering the results of the first nontrivial microscopic (warping) and macroscopic solutions, the third-order warping displacements are found as

$$\begin{aligned}w_1^{(3)}&=\frac{1}{24}\left[4\left(2+\nu\right)y_3^3-h^2\left(6+5\nu\right)y_3\right]v_{3,111}^{(0)}\\&\quad-\bar{a}_0h\left(1+\nu\right)\operatorname{csch}\left(\tfrac{h}{2\sqrt{\bar{a}_0}}\right)\sinh\left(\tfrac{y_3}{\sqrt{\bar{a}_0}}\right)v_{3,111}^{(0)}\ ,\\w_3^{(3)}&=\tfrac{1}{2}\nu\left(y_3^2-\tfrac{h^2}{12}\right)v_{3,11}^{(1)}-\nu y_3v_{1,1}^{(2)}\ .\end{aligned} \tag{38}$$

The second-order stress tensor can be now found by using Eq. (38) and the first nontrivial warping solutions, Eq. (24). The non-local stress tensor (or Cauchy-like stress tensor) is summarized as

$$\begin{aligned}&\sigma_{11}^{(2)}=E\left(v_{1,1}^{(2)}-y_3v_{3,11}^{(1)}\right),\ \sigma_{33}^{(2)}=0,\\&\sigma_{13}^{(2)}=\frac{1}{8}E\left[4y_3^2-h^2-4h\sqrt{\bar{a}_0}\operatorname{csch}\left(\tfrac{h}{2\sqrt{\bar{a}_0}}\right)\cosh\left(\tfrac{y_3}{\sqrt{\bar{a}_0}}\right)\right]v_{3,111}^{(0)}\ .\end{aligned} \tag{39}$$

The local stress tensor (or total stress tensor) is similar to the non-local stress tensor, but the transverse shear stress is different, which is given by

$$t_{13}^{(2)}=\tfrac{E}{8}\left(4y_3^2-h^2\right)v_{3,111}^{(0)}-\bar{a}_0Ev_{3,111}^{(0)}\ . \tag{40}$$

The magnitude of shear stresses at top and bottom surfaces different each other, the total shear stress is more like the stress in a classical elasticity. The non-local stress shows that the surface effect propagates into the bulk (near the surface), whereas the local stress does not. This is not the effect of the pre-stressed state (i.e., the prescribed surface tension) but the through-the-thickness gradient effect. The surface tension as a pre-stressed state does not affect the shear stress distribution, since its derivative with respect to the in-plane coordinate is zero.

The macroscopic beam equation can be derived from Eq. (33), which can be summarized as

$$N^{(2)}\delta v_{1,1}^{(1)}+M^{*(2)}\delta v_{3,11}^{(0)}=0 \tag{41}$$

The solution of Eq. (41) is found to be zero in general, unless there are bending-shear coupling

behavior or special boundary conditions (Kim *et al.* 2008). Thus one can see that the second-order stress state, Eq. (39), is purely described by the solutions of the second-order free energy (or the first nontrivial solutions). The transverse normal stress appears at the fourth-order free energy, which shall be discussed in the following section.

3.2 The fourth-order free energy

The fourth-order energy variation in Eq. (12) can be summarized as follows

$$\begin{aligned}\delta U^{(4)} = &\int_{y_3^-}^{y_3^+} \left(\left(\delta\boldsymbol{\gamma}^{(1)}\right)^T \mathbf{t}^{(3)} + \left(\delta\boldsymbol{\gamma}^{(2)}\right)^T \mathbf{t}^{(2)} + \left(\delta\boldsymbol{\gamma}^{(3)}\right)^T \mathbf{t}^{(1)} \right) dy_3 \\ &+ \left[\bar{a}_0 \left(\delta\boldsymbol{\gamma}^{(1)}\right)^T \boldsymbol{\sigma}_{,3}^{(3)} + \bar{a}_0 \left(\delta\boldsymbol{\gamma}^{(2)}\right)^T \boldsymbol{\sigma}_{,3}^{(2)} + \bar{a}_0 \left(\delta\boldsymbol{\gamma}^{(3)}\right)^T \boldsymbol{\sigma}_{,3}^{(1)} \right]_{y_3^-}^{y_3^+} \\ &+ \left[\bar{a}_0 \left(\delta\boldsymbol{\gamma}^{(1)}\right)^T \boldsymbol{\sigma}_{,1}^{(1)} \right]_{y_1^-}^{y_1^+}\end{aligned} \tag{42}$$

where the third-order total stress vector now includes the axial gradient effect such that

$$\mathbf{t}^{(3)} \equiv \boldsymbol{\sigma}^{(3)} - \bar{a}_0 \boldsymbol{\sigma}_{,33}^{(3)} - \bar{a}_0 \boldsymbol{\sigma}_{,11}^{(1)} \tag{43}$$

Notice here that there is now an axial gradient effect which was not appear at the preceding energy equations. The fourth-order displacement vector has the same form as the third-order one, Eq. (34), and then the third-order strain vector are given by

$$\begin{aligned}\boldsymbol{\gamma}^{(3)} = &\left\lfloor v_{1,1}^{(3)} - y_3 v_{3,11}^{(2)} \quad 0 \quad 0 \right\rfloor^T \\ &+ \left\lfloor 0 \quad w_{3,3}^{(4)} \quad w_{1,3}^{(4)} \right\rfloor^T + \left\lfloor w_{1,1}^{(3)} \quad 0 \quad w_{3,1}^{(3)} \right\rfloor^T\end{aligned} \tag{44}$$

One can find the microscopic and macroscopic equations again by substituting Eq. (44) into Eq. (42). The microscopic equation to be solved is then obtained as

$$\left(t_{13,3}^{(3)} + t_{11,1}^{(2)}\right)\delta w_1^{(2)} = 0, \ \left(t_{33,3}^{(3)} + t_{13,1}^{(2)}\right)\delta w_3^{(2)} = 0, \tag{45}$$

which are subjected to the boundary conditions such that

$$\begin{aligned}&\left(t_{13}^{(3)} - \bar{a}_0 \sigma_{11,13}^{(2)}\right)\delta w_1^{(2)}\Big|_{y_3^-}^{y_3^+} = 0, \ \left(t_{33}^{(3)} - \bar{a}_0 \sigma_{13,13}^{(2)}\right)\delta w_3^{(2)}\Big|_{y_3^-}^{y_3^+} = 0, \\ &\left(\bar{a}_0 \sigma_{13,3}^{(3)}\right)\delta w_{1,3}^{(2)}\Big|_{y_3^-}^{y_3^+} = 0, \ \left(\bar{a}_0 \sigma_{33,3}^{(3)}\right)\delta w_{3,3}^{(2)}\Big|_{y_3^-}^{y_3^+} = 0,\end{aligned} \tag{46}$$

Solving Eq. (45) with Eq. (46) and the warping constraints yields the fourth-order warping displacements as

$$\begin{aligned}w_1^{(4)} = &\frac{1}{24}\left[4\left(2+\nu\right) y_3^3 - h^2 \left(6+5\nu\right) y_3 \right] v_{3,111}^{(1)} \\ &- \bar{a}_0 h \left(1+\nu\right) \operatorname{csch}\left(\tfrac{h}{2\sqrt{\bar{a}_0}}\right) \sinh\left(\tfrac{y_3}{\sqrt{\bar{a}_0}}\right) v_{3,111}^{(1)}, \\ w_3^{(4)} = &\tfrac{1}{2}\nu\left(y_3^2 - \tfrac{h^2}{12} \right) v_{3,11}^{(2)} - \nu y_3 v_{1,1}^{(3)} + \underline{\mathrm{f}\left(a_0, v_{3,1111}^{(0)}\right)},\end{aligned} \tag{47}$$

where the last term (underlined term) in the fourth-order transverse warping displacement is complicate, thus it is omitted here for a brevity.

The third-order stress tensor can be now found by using Eq. (47) and the preceding warping solutions. The non-local stress tensor (or Cauchy-like stress tensor) is summarized as

$$\begin{aligned}
\sigma_{11}^{(3)} &= E\left(v_{1,1}^{(3)} - y_3 v_{3,11}^{(2)}\right) \\
&\quad + \tfrac{E}{24}\left[\nu\left(h^3 - 2h^2 y_3\right) + \left(8y_3^3 - 6h^2 y_3\right)\right] v_{3,1111}^{(0)} \\
&\quad + \overline{a}_0 \tfrac{E}{2}\left[\nu h - 2h(1+\nu)\,\mathrm{csch}\left(\tfrac{h}{2\sqrt{\overline{a}_0}}\right)\sinh\left(\tfrac{y_3}{\sqrt{\overline{a}_0}}\right)\right] v_{3,1111}^{(0)}, \\
\sigma_{13}^{(3)} &= \tfrac{E}{48(1+\nu)}\left[12\left(2+\nu\right)y_3^2 - h^2\left(6+5\nu\right)\right] v_{3,111}^{(1)} \\
&\quad - \tfrac{1}{2}\sqrt{\overline{a}_0}\,Eh\,\mathrm{csch}\left(\tfrac{h}{2\sqrt{\overline{a}_0}}\right)\cosh\left(\tfrac{y_3}{\sqrt{\overline{a}_0}}\right) v_{3,111}^{(1)}, \\
\sigma_{33}^{(3)} &= \tfrac{E}{24}\left(h - y_3\right)\left(h + 2y_3\right)^2 v_{3,1111}^{(0)} + \tfrac{1}{2}\overline{a}_0 Eh v_{3,1111}^{(0)}.
\end{aligned} \tag{48}$$

The local stress tensor can be calculated by Eq. (43), which is obtained as

$$\begin{aligned}
t_{11}^{(3)} &= E\left(v_{1,1}^{(3)} - y_3 v_{3,11}^{(2)}\right) + \overline{a}_0 \tfrac{E}{2}\left(\nu h - 2y_3\right) v_{3,1111}^{(0)} \\
&\quad + \tfrac{E}{24}\left[\nu\left(h^3 - 2h^2 y_3\right) + \left(8y_3^3 - 6h^2 y_3\right)\right] v_{3,1111}^{(0)} \\
&\quad + \tfrac{1}{2}\overline{a}_0 E(\nu h - 2y_3) v_{3,1111}^{(0)}, \\
t_{13}^{(3)} &= \tfrac{E}{48(1+\nu)}\left[12\left(2+\nu\right)y_3^2 - h^2\left(6+5\nu\right)\right] v_{3,111}^{(1)} - \tfrac{1}{2}\overline{a}_0 E\,\tfrac{(2+\nu)}{(1+\nu)} v_{3,111}^{(1)}, \\
t_{33}^{(3)} &= \tfrac{E}{24}\left(h - y_3\right)\left(h + 2y_3\right)^2 v_{3,1111}^{(0)} + \tfrac{1}{2}\overline{a}_0 E\left(h + 2y_3\right) v_{3,1111}^{(0)}.
\end{aligned} \tag{49}$$

In both non-local and local stresses, the transverse shear stresses become zeros, since the solutions of the third-order energy macroscopic problem, Eq. (41), are zeros in many cases.

The macroscopic beam equation can be derived from Eq. (42), which can be summarized as

$$\begin{aligned}
&N^{(3)}\delta v_{1,1}^{(1)} \\
&+\left[M^{*(3)} + \overline{a}_0\left(\nu + \sqrt{\overline{a}_0}\,\tfrac{12}{h}(1+\nu)\coth\left(\tfrac{h}{2\sqrt{\overline{a}_0}}\right)\right) M_{,11}^{(1)}\right]\delta v_{3,11}^{(0)} = 0
\end{aligned} \tag{50}$$

This has solutions unlike the preceding macroscopic equations. The third-order stress resultants include the first nontrivial macroscopic solutions, Eq. (32). The in-plane stress resultants are then explicitly given as

$$N^{(3)} = EAv_{1,1}^{(3)} + \left(\tfrac{h}{2}\nu + \overline{a}_0\,\tfrac{6}{h}\right) M_{,11}^{(1)} \tag{51}$$

which has the solution if the second-order derivative of the first-order bending moment is not zero. This happens when the beam is subjected to a distributed transverse load. To complete the solution, one needs to consider the governing equation and associated boundary conditions. They are expressed as

$$-\int_{y_1^-}^{y_1^+}\left(N_{,1}^{(3)}\delta v_1^{(1)}\right)dy_1+\left[N^{(3)}\delta v_1^{(1)}\right]_{y_1^-}^{y_1^+}+\underline{\left[\bar{a}_0 N_{,1}^{(1)}\delta v_{1,1}^{(1)}\right]_{y_1^-}^{y_1^+}}=0, \tag{52}$$

in which the first term is the governing equation, the second term is the boundary condition, and the last term is the surface effect at both end of the beam. The first-order stress resultant is already known, and therefore it acts like the external loading. In this case, there is no external physical load since it is already considered in the first-order stress resultant, Eq. (30). Thus the solutions of Eq. (52) are affected by the fictive internal volume force (Kim *et al.* 2008) and axial strain gradient effect.

The moment governing equation and boundary conditions are given as follows

$$\begin{aligned}&-\int_{y_1^-}^{y_1^+} M_{,11}^{*(3)}\delta v_3^{(0)}dy_1\\&+\left[M^{*(3)}\delta v_{3,1}^{(0)}\right]_{y_1^-}^{y_1^+}-\left[M_{,1}^{*(3)}\delta v_3^{(0)}\right]_{y_1^-}^{y_1^+}+\underline{\left[\bar{a}_0 M_{,1}^{(1)}\delta v_{3,11}^{(0)}\right]_{y_1^-}^{y_1^+}}=0,\end{aligned} \tag{53}$$

where the underlined term represents the surface effect, which is similar to that in Eq. (52). The explicit form of the third-order bending moment is expressed by

$$\begin{aligned}M^{*(3)}\equiv EI\left[1+\bar{a}_0\tfrac{12}{h^2}\right]v_{3,11}^{(2)}+\tfrac{h^2}{60}\left(12+5\nu\right)M_{,11}^{(1)}\\+\bar{a}_0\left(1+\nu\right)\left[1+\sqrt{\bar{a}_0}\tfrac{12}{h}\coth\left(\tfrac{h}{2\sqrt{\bar{a}_0}}\right)\right]M_{,11}^{(1)}\end{aligned} \tag{54}$$

In contrast to this, the bending moment by the total stress is given as

$$M^{(3)}=EIv_{3,11}^{(2)}+\tfrac{h^2}{60}\left(12+5\nu\right)M_{,11}^{(1)}+\bar{a}_0 M_{,11}^{(1)} \tag{55}$$

in which the bending moment stiffness is the same as that of a classical elasticity, the second term is a transverse loading effect, and the last term is a strain-gradient effect in the average sense.

4. Numerical examples and discussion

In this section, a cantilevered nano-beam is taken as a test-bed to investigate the through-the-thickness distributions of both Cauchy-like stress and total stress. For the purpose of comparative studies, material properties including surface characteristics are considered, which are reported in literature (Gurtin and Murdoch 1978, Lu *et al*. 2006). Numerical results are obtained for two loading conditions. One is subjected to an axial force at the free end of the beam, and the other is subjected to a uniform pressure on the top surface of the beam.

4.1 Surface stress state

According to Gurtin and Murdoch (1975, 1978), the surface constitutive and equilibrium equations, for one-dimensional case, can be expressed as

$$\tau_{11}^{\pm}=\tau_0+\left(\lambda_0+2\mu_0\right)\gamma_{11}^{\pm},\quad \tau_{11,1}^{+}-\sigma_{13}^{+}=0,\ \ \tau_{11,1}^{-}+\sigma_{13}^{-}=0, \tag{56}$$

Table 1 Example material properties

Properties	Young's modulus	Poisson's ratio, ν	Residual surface tension, τ_0	Surface Lame constant, λ_0	Surface Lame constant, μ_0
Bulk	56.25 GPa	0.25	-	-	-
Surface	-	-	110 N/m	7×10^3 N/m	8×10^3 N/m

where the superscript '+' and '–'denotes the top surface and bottom surface of the beam, respectively. The residual surface tension is denoted by τ_0, and λ_0 and μ_0 represent the surface Lame constants. These surface properties are listed in Table 1.

One can estimate the transverse shear stress at the top and bottom surfaces of the bulk by employing an Euler-Bernoulli beam theory. The shear force generated by the surface stress is calculated as

$$\begin{aligned} Q &= \tfrac{h}{2}\left(\tau_{11,1}^{+} - \tau_{11,1}^{+}\right) = \tfrac{h}{2}\left(t_{13}^{(2)+} + t_{13}^{(2)-}\right) = \left\langle \sigma_{13}^{(2)} \right\rangle \\ &= -\tfrac{1}{2}h^2\left(\lambda_0 + 2\mu_0\right)v_{3,111}^{(0)} \end{aligned} \tag{57}$$

The shear force can be matched with the shear force computed by the second-order shear stresses given in Eqs. (39) and (40). Taking the nonlocal contribution, one can then estimate the internal length scale parameter 'a_0' in such a way that

$$-\tfrac{1}{2}h^2\left(\lambda_0 + 2\mu_0\right)v_{3,111} = -\bar{a}_0 E h v_{3,111}^{(0)} \rightarrow \bar{a}_0 = \frac{h\left(\lambda_0 + 2\mu_0\right)}{2E} \tag{58}$$

This is however not able to take into account the through-the-thickness distribution of the surface stress state. In order to consider it, the shear stress at top and bottom surfaces may be directly matched with the surface stress by neglecting the in-plane strain contribution. That is

$$\sigma_{13}^{\pm} = \sigma_{13}^{(2)\pm} \rightarrow \sqrt{\bar{a}_0} = \frac{\left(\lambda_0 + 2\mu_0\right)}{E}\tanh\left(\tfrac{h}{2\sqrt{\bar{a}_0}}\right) \tag{59}$$

It is a nonlinear equation for the internal length scale parameter to be calculated. The upper and lower limits of Eq. (58) can be estimated as

$$\bar{a}_0^{U} = \frac{h\left(\lambda_0 + 2\mu_0\right)}{2E}\ \left(\text{as } h \rightarrow 0\right),\ \ \bar{a}_0^{L} = \frac{\left(\lambda_0 + 2\mu_0\right)^2}{E^2}\ \left(\text{as } h \rightarrow \infty\right) \tag{60}$$

Eq. (59) implies that the parameter should be positive. In order to consider the softening effect, one may need to employ a second strain gradient theory, which will be subjected to future work. For the given material properties, the internal length scale parameter is estimated by

$$\sqrt{\bar{a}_0} = \frac{\left(\lambda_0 + 2\mu_0\right)}{E} = 0.409\ nm \tag{61}$$

One can now see the through-the-thickness stress distribution due to the residual surface tension. The distributions, which is calculated by using Eq. (27), are illustrated in Fig. 1, where the beam thickness varies from 5 nm to 40 nm. For comparison purpose, the distribution with the

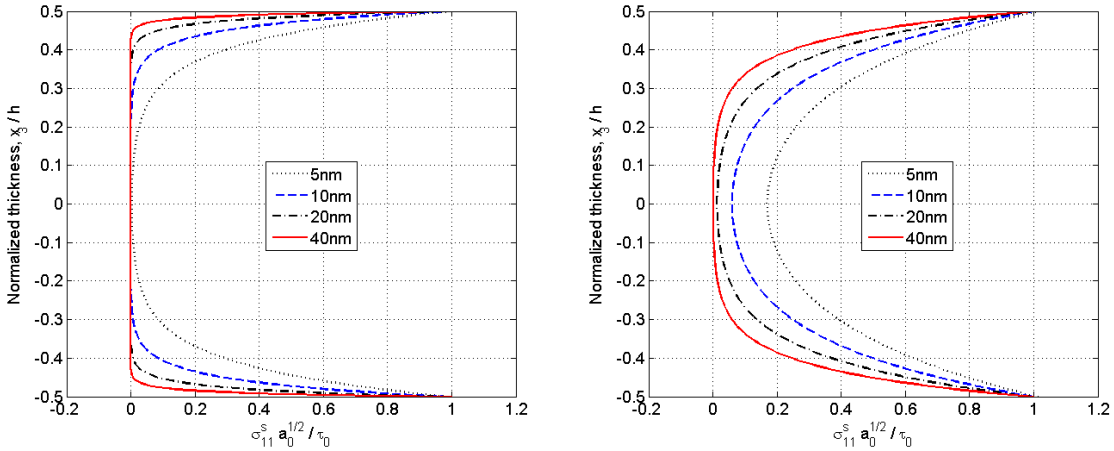

(a) With the lower limit (b) With the upper limit

Fig. 1 The normalized through-the-thickness stress distribution due to the residual surface tension

upper limit is also plotted in Fig. 1(b), in which it is observed that the internal length scale parameter plays a significant role in the stress distribution. It is reasonable to use the lower limit of the parameter, since we made an assumption that the beam thickness is relatively large as compare to the parameter. For this reason, henceforth the lower limit value shall be used in numerical examples.

4.2 Cantilevered beam under axial force

The beam subjected to an axial force is considered first, in order to investigate the residual surface tension effect to the through-the-thickness distribution of a normal stress. The beam governing equation and associated boundary conditions are given in Eq. (30). Applying the force to the end of the beam causes a complicate internal normal stress state. A nano-beam is generally slender, thus one can make an assumption that the stress developed by the axial force is constant over the cross-section of the beam at considerable distances from the edge of the beam. For the residual surface tension, however, there is no such distance to decay. Therefore one may not apply the Saint-Venant's principle, which enforces us to consider the through-the-thickness distribution with the residual stress. For instance, there are tensile and compressive stresses through the thickness of the beam. It is possible to develop a negative stress while the stress near the surface is positive, if the stress in Eq. (27) is less than zero at the middle of the beam such that

$$\sigma_{11}^{(2)}\Big|_{y_3=0} = \frac{p_1 - 2\tau_0}{h} + \frac{\tau_0 h}{\sqrt{\bar{a}_0}}\operatorname{csch}\left(\frac{h}{2\sqrt{\bar{a}_0}}\right) < 0 \tag{62}$$

The stress distributions subjected to tensile or compressive loads are illustrated in Fig. 2, where the beam width is assumed to be 40 nm, and the beam thickness varies 5 nm to 40 nm. The magnitude of applied forces is assumed to be 20 μN, and thus the force per unit width (p_1) is 500 N/m, which is the same order of magnitude as the residual surface tension (τ_0=110 N/m). There is a negative stress even for a tension, if the applied force is less than 8 μN. For the compressive load

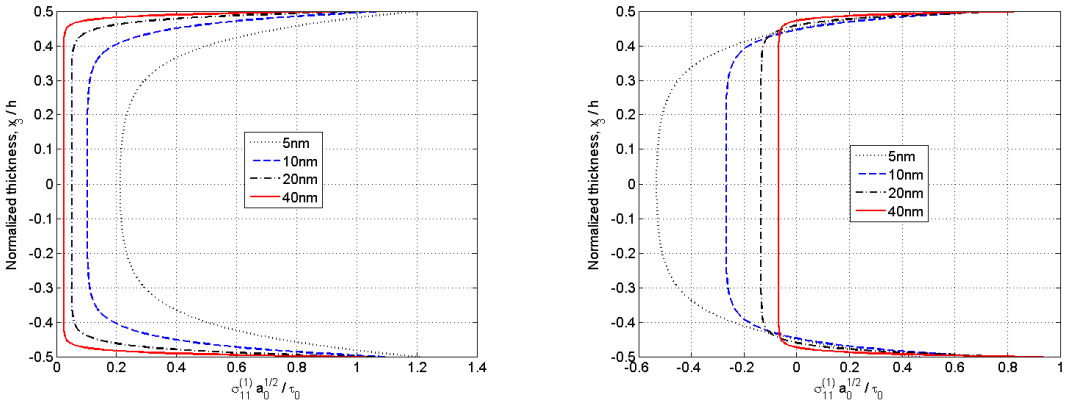

(a) Tensile force 20 μN (b) Compressive force -20 μN

Fig. 2 The normalized through-the-thickness stress distribution under axial forces at the free end

case, the residual surface stress is still dominant near the surfaces. In order to have negative stresses all over the thickness for the case of the beam with 40 nm thickness, the magnitude of applied force should be larger than 400 μN.

4.3 Cantilevered beam under uniform transverse pressure

The beam subjected to a uniform transverse pressure is considered, in order to investigate the surface stress effect to the through-the-thickness distribution of transverse stresses. In a first strain gradient elasticity, the surface stress is automatically captured by the strain gradient, which is known as 'Gurtin-Murdoch traction' at the surface of an elastic body (Polizzotto 2012). These stress conditions are presented in Eq. (37) for the second-order total stress tensor and in Eq. (46) for the third-order total stress tensor. The transverse stresses can be calculated by higher-order free energies, the shear stress is obtained by the third-order energy and the transverse normal stress by the fourth-order energy.

The total and Cauchy-like shear stresses, from Eqs. (39)-(40), can be summarized as follows

$$\begin{aligned} t_{13}^{(2)} &= \tfrac{E}{8}\left(4y_3^2 - h^2\right)v_{3,111}^{(0)} - \bar{a}_0 E v_{3,111}^{(0)}\ , \\ \sigma_{13}^{(2)} &= \tfrac{E}{8}\left[4y_3^2 - h^2 - 4h\sqrt{\bar{a}_0}\,\mathrm{csch}\left(\tfrac{h}{2\sqrt{\bar{a}_0}}\right)\cosh\left(\tfrac{y_3}{\sqrt{\bar{a}_0}}\right)\right]v_{3,111}^{(0)}\ , \end{aligned} \tag{63}$$

where the zeroth-order transverse displacement for the uniform pressure (p_3) is obtained as:

$$v_3^{(0)} = \frac{p_3 b}{24EI}\, y_1^{\,2}\left(y_1^2 - 4y_1 L + 6L^2\right), \tag{64}$$

in which 'L' is the length of the beam. The shear stress at the root (i.e., y_1=0) can be expressed in terms of the pressure as follows

$$\begin{aligned} t_{13}^{(2)} &= p_3 L\,\tfrac{6}{h}\left[2\bar{a}_0 - \left(y_3^2 - \tfrac{h^2}{4}\right)\right]\left(\tfrac{1}{h^2}\right), \\ \sigma_{13}^{(2)} &= p_3 L\,\tfrac{6}{h}\left[h\sqrt{\bar{a}_0}\,\mathrm{csch}\left(\tfrac{h}{2\sqrt{\bar{a}_0}}\right)\cosh\left(\tfrac{y_3}{\sqrt{\bar{a}_0}}\right) - \left(y_3^2 - \tfrac{h^2}{4}\right)\right]\left(\tfrac{1}{h^2}\right), \end{aligned} \tag{65}$$

The shear stresses are non-dimensionalized, which are plotted through the thickness of the beam as shown in Fig. 3. The total stress in Fig. 3(a) and Cauchy-like stress in Fig. 3(b) show different distributions qualitatively. Although the shear force by both stress is equivalent, the Cauchy-like stress magnitude is much larger than the total stress near the surfaces.

Following the same way described in the above, the transverse normal stresses, from Eqs. (48)-(49), can be obtained as follows

$$\begin{aligned} t_{33}^{(3)} &= \frac{q}{2h^3}\left[\left(h-y_3\right)\left(h+2y_3\right)^2+12\bar{a}_0\left(h+2y_3\right)\right], \\ \sigma_{33}^{(3)} &= \frac{q}{2h^3}\left[\left(h-y_3\right)\left(h+2y_3\right)^2+12\bar{a}_0 h\right], \end{aligned} \tag{66}$$

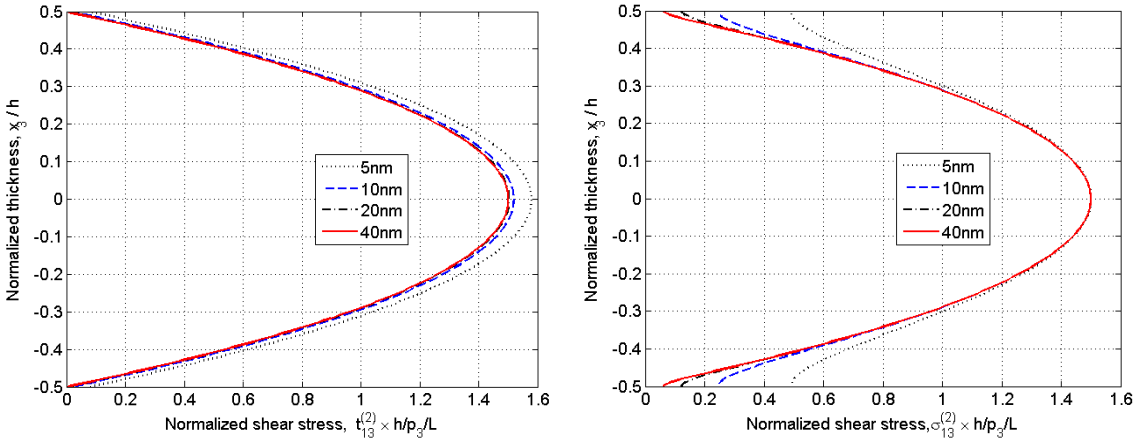

(a) Total shear stress (b) Cauchy-like shear stress

Fig. 3 The normalized through-the-thickness shear stress distribution under a uniform pressure

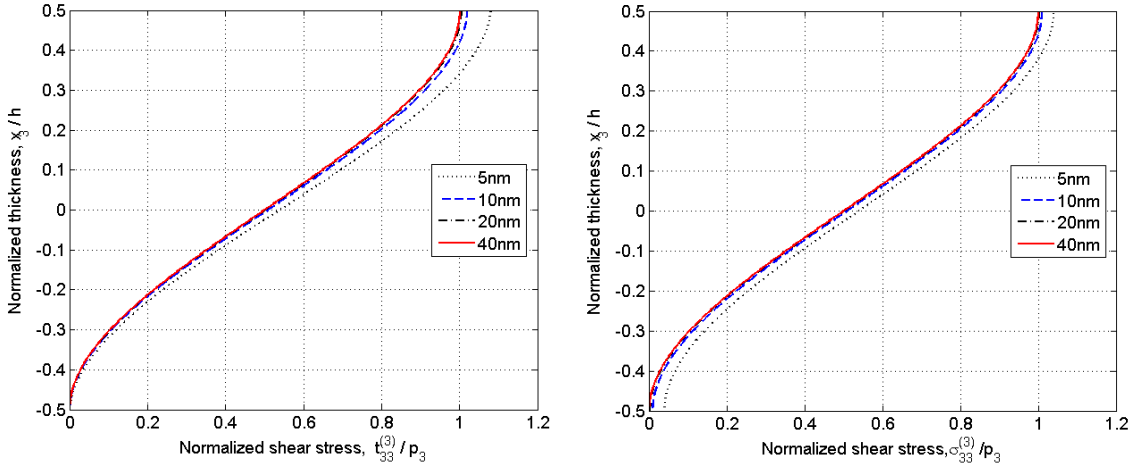

(a) Total stress (b) Cauchy-like stress

Fig. 4 The normalized transverse normal stress distribution under a uniform pressure

These stresses are illustrated in Fig. 4, where the magnitude is normalized by the pressure density p_3. The total stress at the bottom surface is zero, whereas the Cauchy-like stress is not. This is because the total stress cannot simultaneously satisfy the conditions at both surfaces. The Cauchy-like stress (or nonlocal stress) is able to simulate the tensile stress due to the surface effect at the surfaces. The surface stress contribution to the normal stress distribution is relatively small as compared to the shear stress (Fig. 3).

On the other hand, the third-order in-plane normal stress is strongly affected by the residual surface tension unless a high pressure is applied. However the pressure causes very large deflection at the free end of the beam, which leads to a geometrically nonlinear formulation. This is on-going research work and shall be treated in another paper.

5. Conclusions

Nano-beam models are derived based on a first strain gradient elasticity by employing a systematic asymptotic expansion method. Unlike many research works reported in literature, it is demonstrated that the thickness length scale effect is more important than the axial length scale effect for beam- and/or plate-like structures. The present asymptotic formulation reveals that there exists the surface stress effect even for a fundamental beam formulation. This effect is systematically connected to the next order shear stress, in which the stresses at top and bottom surfaces are prescribed by the first-order stresses. Contributions made in this paper can be summarized as follows:

• Systematic dimensional reduction from three-dimensional strain gradient elasticity to beam models by employing a formal asymptotic expansion method

• The models obtained indicate that a major source of size-effect comes from the surface shear stress that is smeared into the bending stiffness in an Euler-Bernoulli-like beam model. The effect makes the beam stiffer.

• The unknown length scale parameter is systematically matched with the result reported in literature, in which the Cauchy-like shear stress is connected to the surface constitutive equation by Gurtin and Murdoch (1978).

• The parameter plays a crucial role in the bending stiffness and the through-the-thickness distributions of stresses. It is shown that the order of the internal parameter is similar to that of a lattice constant. A second strain elasticity model may be needed to explore the softening size effect, since the strain gradient elasticity considered in this paper cannot explain the softening behavior.

• The residual surface stress state has an impact on the stress distribution in both axial and transverse deformation problems. The higher-order in-plane normal stress, the third-order stress in this paper, is strongly affected by the residual stress. In order to properly formulate, one may need to consider a geometrically nonlinear strain gradient elasticity.

References

Mindlin, R.D. (1964), “Micro-structure in linear elasticity”, *Arch. Rat. Mech. Anal.*, **16**(1), 51-78.

Mindlin, R.D. (1965), “Second gradient of strain and surface-tension in linear elasticity”, *Int. J. Solids Struct.*, **1**(4), 417-438.

Eringen, A.C. (1983), "On differential equations of nonlocal elasticity and solutions of screw dislocation and surface waves", *J. Appl. Phys.*, **54**(9), 4703-4710.
Eringen, A.C. (2002), *Nonlocal Continuum Field Theories*, Springer-Verlag New York, Inc.
Kim, W. and Cho, M. (2010), "Surface effect on the self-equilibrium state and size-dependent elasticity of FCC thin films", *Modelling Simul. Mater. Sci. Eng*., **18**(8), 085006.
Peddieson, J., Buchanan, G.G. and McNitt, R.P. (2003), "Application of nonlocal continuum models to nanotechnology", *Int. J. Eng. Sci.*, **41**(3), 305-312.
Wang, C.M., Zhang, Y.Y., Ramesh, S.S. and Kitipornchai, S. (2006), "Buckling analysis of micro- and nano-rods/tubes based on nonlocal Timoshenko beam theory", *J. Phys. D: Appl. Phys*., **39**(17), 3904-3909.
Reddy, J.N. (2007), "Nonlocal theories for bending, buckling and vibration of beams", *Int. J. Eng. Sci.*, **45**(2), 288-307.
Kim, J.-S. (2014a), "Application of nonlocal models to nano beams, part I: axial length scale effect", *J. Nanosci. Nanotechnol.*, **14**(10), 7592-7596.
Yang, F., Chong, A.C.M., Lam, D.C.C. and Tong, P. (2002), "Couple stress based strain gradient theory for elasticity", *Int. J. Solids Struct*., **39**(10), 2731-2743.
Lam, D.C.C., Yang, F., Chong, A.C.M., Wang, J. and Tong, P. (2003), "Experiments and theory in strain gradient elasticity", *J. Mech. Phys. Solid.*, **51**(8), 1477-1508.
Ma, H.M., Gao, X.-L. and Reddy, J.N. (2008), "A microstructure-dependent Timoshenko beam model based on a modified couple stress theory", *J. Mech. Phys. Solid.*, **56**(12), 3379-3391.
Gurtin, M.E. and Murdoch, A.I. (1975), "A continuum theory of elastic material surfaces", *Arch. Rat. Mech. Anal*., **57**(4), 291-323.
Gurtin, M.E. and Murdoch, A.I. (1978), "Surface stress in solids", *Int. J. Solid Struct.*, **14**(6), 431-440.
Lim, C.W. and He, L.H. (2004), "Size-dependent nonlinear response of thin elastic films with nano-scale thickness", *Int. J. Mech. Sci.*, **46**(11), 1715-1726.
Lu, P., He, L.H., Lee, H.P. and Lu, C. (2006), "Thin plate theory including surface effects", *Int. J. Solid Struct.*, **43**(16), 4631-4647.
Kim, J.-S. (2014b), "Application of nonlocal models to nano beams, part II: thickness length scale effect", *J. Nanosci. Nanotechnol.*, **14**(10), 7597-7602.
Cho, M., Choi, J. and Kim, W. (2009), "Continuum-based bridging model of nanoscale thin film considering surface effects", *Jap. J. Appl. Phys.*, **48**(2R), 020219.
Kim, W., Rhee, S.Y. and Cho, M. (2012), "Molecular dynamics-based continuum models for the linear elasticity of nanofilms and nanowires with anisotropic surface effects", *J. Mech. Mater. Struct.*, **7**(7), 613-639.
Lazar, M., Maugin, G.A. and Aifantis, E.C. (2006), "Dislocations in second strain gradient elasticity", *Int. J. Solid Struct.*, **43**(6), 1787-1817.
Polizzotto, C. (2012), "A gradient elasticity theory for second-grade materials and higher order inertia", *Int. J. Solid Struct.*, **49**(15), 2121-2137.
Polizzotto, C. (2003), "Gradient elasticity and nonstandard boundary conditions", *Int. J. Solids Struct.*, **40**(26), 7399-7423.
Polizzotto, C. (2015), "A unifying variational framework for stress gradient and strain gradient elasticity theories", *Euro. J. Mech. A/Solid.*, **49**, 430-440.
Di Paola, M., Pirrotta, A. and Zingales, M. (2010), "Mechanically-based to non-local elasticity: Variational principles", *Int. J. Solid Struct.*, **47**(5), 539-548.
Askes, H. and Aifantis, E.C. (2011), "Gradient elasticity in statics and dynamics: An overview of formulations, length scale identification procedure, finite element implementations and new results", *Int. J. Solid Struct.*, **48**(13), 1962-1990.
Kim, J.-S., Cho, M. and Smith, E.C. (2008), "An asymptotic analysis of composite beams with kinematically corrected end effects", *Int. J. Solid Struct.*, **45**(7), 1954-1977.
Kim, J.-S. (2009), "An asymptotic analysis of anisotropic heterogeneous plates with consideration of end effects", *J. Mech. Mater. Struct.*, **4**(9), 1535-1553.

Kim, J.-S. and Wang, K.W. (2011), "On the asymptotic boundary conditions of an anisotropic beam via virtual work principle", *Int. J. Solid Struct.*, **48**(16-17), 2422-2431.

MC